

# Engineering Notes

ENGINEERING NOTES are short manuscripts describing new developments or important results of a preliminary nature. These Notes cannot exceed 6 manuscript pages and 3 figures; a page of text may be substituted for a figure and vice versa. After informal review by the editors, they may be published within a few months of the date of receipt. Style requirements are the same as for regular contributions (see inside back cover).

## Topology Optimization of Transport Wing Internal Structure

Vladimir O. Balabanov\* and Raphael T. Haftka†  
Virginia Polytechnic Institute and State University,  
Blacksburg, Virginia 24061

### Introduction

THE problem of designing efficient wing internal structure for a high speed civil transport (HSCT), i.e., of determining the overall arrangement of spars and ribs, is considered. Once the arrangement and number of ribs and spars has been determined the design problem reduces to standard sizing structural optimization. However, determining the number of spars and ribs and the overall concept of their arrangement is a topology optimization problem.

The optimization was performed by an optimization program developed by Ben-Tal and Bendsøe.<sup>1</sup> To avoid prohibitive computational requirements, topology optimization is often performed for the idealized design problem of obtaining a minimum compliance (maximum stiffness) structure. Here we introduced the additional simplification of modeling the wing as a truss structure. The ground structure approach was used for the optimization.

The ground structure approach for a truss structure begins with a dense set of nodal points and nonoverlapping member connections between them. This set of member connections is called the ground structure. The optimal topology is a subset of the initial ground structure and is obtained by varying the cross-sectional areas of the members and eliminating unneeded members.

For two-dimensional structures it is common to connect every node to every other node. This leads to a very large number of members. Because we cannot afford such a strategy for a complex three-dimensional structure representing the wing of the HSCT, we only connected each node of the ground structure to its eight nearest neighbor nodes on the same wing surface and to nine more neighboring nodes on the other wing surface.

We wanted to check how fuselage flexibility affects the topology of the internal structure, and so we compared two cases of rigid and flexible fuselage. For both cases, the load applied, corresponding to symmetric pull-up maneuver, was the same. It was lumped into nodal forces including only components in the  $z$  direction. The load was composed of

aerodynamic forces and inertia forces due to the distributed weight of the structure, nonstructural items, and fuel. Additional details about load determination for this case are given in Refs. 2 and 3. The weights of the fuselage and of the wing were the same for both cases.

### Results

#### Aircraft with Rigid Fuselage

For this case the wing was cantilevered; the ground structure representing this case includes 149 nodes and 964 bars connecting them with the distributed load lumped at 121 nodes. (Forces were not applied at the boundary nodes in the plane of symmetry.)

The optimal structure has a relative compliance of 12.33% compared to the ground structure (i.e., it is eight times stiffer). Bars of the optimal structure were divided into three groups according to individual bar volumes  $V_i$ . Bars with volumes in the range from  $\max\{V_i\}/10$  to  $\max\{V_i\}$  are called main bars. In this case main bars accounted for 97.9% of the given volume  $V_w$  of the material in the wing structure. They are shown in Fig. 1. More details about the ground structure and the optimal design are presented in Ref. 2.

#### Aircraft with Flexible Fuselage

Since here we are interested in the wing internal structure, but not in that of the fuselage, we assume that the fuselage structure is given and does not change during the optimization process. We modeled the fuselage with 74 nodes and 246 bars. The ground structure of the wing was the same as before. The whole ground structure consists of 193 nodes and 1146 bars.

With the part of the ground structure fixed, the ratio of the variable part (wing) to the fixed part (fuselage) is important. We estimated this ratio as 0.81 on the basis of a finite element model of a NASA baseline design used by Hutchison et al.<sup>3</sup>

Three points at each of the two ends of the fuselage were fixed, because due to very slow convergence it was impossible to obtain the optimum design when only points near the c.g. were fixed. These boundary conditions are not totally compatible with the type of deformations expected in the flight, but nevertheless they allow the fuselage to deform under distributed load. The distributed load was lumped at the remaining 187 nodes.

The optimal structure in this case has a relative compliance of 84.25% compared to the ground structure (i.e., a factor of 1.19 increase in stiffness). The main bars, accounting for 95.7% of  $V_w$ , are shown in Fig. 2. In the optimal structure bars with large volumes are located along the fuselage. This may be considered as an attempt to use the wing structure to stiffen the flexible fuselage structure.

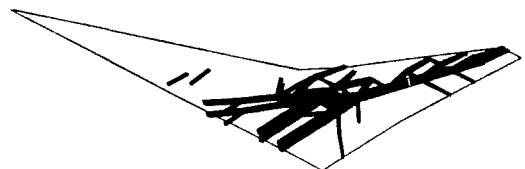


Fig. 1 Main bars for HSCT wing optimal design; rigid fuselage.

Received Jan. 25, 1995; revision received June 21, 1995; accepted for publication June 29, 1995. Copyright © 1995 by V. O. Balabanov and R. T. Haftka. Published by the American Institute of Aeronautics and Astronautics, Inc., with permission.

\*Graduate Research Assistant. Student Member AIAA.

†Christopher C. Kraft Professor, Department of Aerospace and Ocean Engineering and Multidisciplinary Analysis and Design (MAD) Center for Advanced Vehicles; currently at the Department of Aerospace Engineering, Mechanics and Engineering Science, University of Florida, Gainesville, FL 32611. Associate Fellow AIAA.

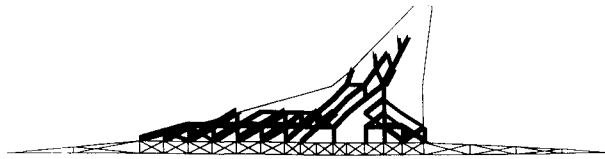


Fig. 2 Main bars for HSCT wing optimal design; flexible fuselage.

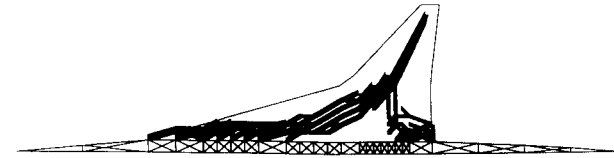


Fig. 3 Main bars for HSCT wing optimal design; flexible fuselage; refined mesh.

#### Effect of Mesh Density

Our next step was to investigate the effect of mesh density for the HSCT model with flexible fuselage. The mesh used in the previous step was refined. The refined ground structure consists of 436 nodes and 3015 bars. 180 nodes and 337 bars of this ground structure were used to define the fuselage. The weights of the fuselage and of the wing and the boundary conditions were the same as for the less refined mesh. The same total load was distributed now at 430 nodes (again, all nodal points except for the six fixed ones).

The optimal structure for this case has a relative compliance of 77.39% compared to the ground structure (i.e., a factor of 1.29 increase in stiffness).

The main bars, accounting for 90.6% of  $V_w$ , are shown in Fig. 3. Comparison with the results obtained for the coarser mesh shows that the location of the main bars is almost the same.

#### Conclusions

The problem of designing efficient wing internal structure for the HSCT was considered. The ground structure approach with an algorithm due to Ben-Tal and Bendsøe<sup>1</sup> was used to solve this problem. The main simplifying assumptions were modeling the aircraft internal structure as a truss and using compliance as a single criterion for the design. In spite of these simplifications we hope that the results obtained provide an indication of the kind of internal structure required for the HSCT wing.

Based on the results of the work described in this Note we may conclude the following:

- 1) Compliance minimization based on ground structure approach is feasible for three-dimensional structures, but requires reduced connectivity to reduce the number of bars.
- 2) Fuselage flexibility has a large effect on topology, especially in the inboard wing area.
- 3) Refining the mesh and the load distribution did not lead to substantial changes in topology.

#### Acknowledgment

This work was supported by NASA Grant NAG1-168.

#### References

- <sup>1</sup>Ben-Tal, A., and Bendsøe, M. P., "A New Method for Optimal Truss Topology Design," *SIAM Journal on Optimization*, Vol. 3, No. 2, 1993, pp. 322-358.
- <sup>2</sup>Balabanov, V. O., and Haftka, R. T., "Topology Optimization of Transport Wing Internal Structure," AIAA Paper 94-4414, Sept. 1994.
- <sup>3</sup>Hutchison, M. G., Huang, X., Mason, W. H., Haftka, R. T., and Grossman, B., "Variable-Complexity Aerodynamic-Structural Design of a High-Speed Civil Transport Wing," AIAA Paper 92-4695, Sept. 1992.

## Analytic $V$ Speeds from Linearized Propeller Polar

John T. Lowry\*

Flight Physics, Billings, Montana 59104-0919

#### Introduction

THE primary fixed-pitch, propeller-driven, normally aspirated aircraft flight performance  $V$  speeds (best angle of climb speed  $V_x$ , best rate of climb speed  $V_y$ , maximum level speed  $V_m$ ) are given by simple analytic expressions when ordinary power-available/power-required ( $P_{av}/P_{rc}$ ) analysis is combined with the assumption<sup>1</sup> of linearity of the propeller polar:  $C_T/J^2 = mC_p/J^2 + b$ . Constants  $m$  and  $b$  can be obtained from propeller charts or by flight tests. (Because we often know more about power than thrust, we have reversed, relative to Von Mises's usage, the independent and dependent variables.) We also require an expression for the drop in engine torque  $M$  with relative atmospheric density  $\sigma$ , from its standard mean sea level (MSL) value  $M_0$ ; we use essentially that of Gagg and Farrar<sup>2</sup>:  $M(\sigma) = \phi(\sigma)M_0 = M_0(\sigma - C)/(1 - C)$ .  $C$  is in the range  $[0.11, 0.15]$  and can be obtained from the usual engine chart or approximated (Gagg and Farrar's value was 0.117) as 0.12. We focus on torque, rather than on brake power, because torque is nearly constant at constant throttle position (or manifold absolute pressure) and altitude. A few pieces of operating handbook data on the aircraft are needed, as is a drag polar for the configuration under consideration. The simplicity of the resulting expressions may be useful in preliminary flight testing and as a pedagogical tool for students of aircraft performance.

These ideas share motivation and basic features with Ref. 1, Chapter XV. Major differences between our treatments are as follows:

- 1) His dimensionless variables are less transparent than our manifestly engineering ones.
- 2) He uses a representative propeller blade element in place of our focus on the linearized polar parameters.
- 3) He requires several arguments concerning small quantities or neglected terms of second order while we need not do so.
- 4) Some of his results are series expansions while ours are all in closed form.

The straightforwardness of the development discussed next allows it to not only derive simple formulas for the various full-throttle  $V$  speeds (as functions of gross aircraft weight  $W$  and atmospheric density  $\rho$ ), but also such results as 1) the independence of  $V_x$ , in calibrated terms, of density altitude and 2) formulas connecting  $V_x$ ,  $V_y$ , and  $V_m$  (all at the same  $W$  and  $\rho$ ). The necessity of that latter result can be argued for by simply counting unknown parameters and given relations.

With a few additional assumptions, and recording of revolutions per minute data, this work can be extended to partial-throttle performance, to takeoff and landing performance, and to constant-speed propeller operation. We won't make those extensions here. Its small number of assumptions gives this treatment a boundedness that may keep the student from being sidetracked. Armed with an ordinary spreadsheet program he or she can easily generate concrete graphs or tables showing a given airplane's steady flight characteristics.

Received Jan. 28, 1995; revision received July 1, 1995; accepted for publication July 1, 1995. Copyright © 1995 by J. T. Lowry. Published by the American Institute of Aeronautics and Astronautics, Inc., with permission.

\*Owner, 724 Alderson Avenue, P.O. Box 20919.